

Signature of the transition to a bound state in thermoelectric quantum transport

Étienne Jussiau,^{1,*} Masahiro Hasegawa,^{2,†} and Robert S. Whitney^{1,‡}

¹*Université Grenoble-Alpes, CNRS, LPMMC, 38000 Grenoble, France*

²*Institute for Solid State Physics, The University of Tokyo, Kashiwa, Chiba 277-8581, Japan*

(Dated: November 28, 2018)

We study a quantum dot coupled to two semiconducting reservoirs, when the dot level and the electrochemical potential are both close to a band edge in the reservoirs. This is modelled with an exactly solvable Hamiltonian without interactions (the Fano-Anderson model). The model shows an abrupt transition in its physics as the dot-reservoir coupling is increased, if the band's density of states goes to zero at the band edge. Then an infinite-lifetime bound state appears in the band gap, when the coupling is stronger than a critical value. We study the signature of this transition in the electric and thermoelectric responses, showing that they change very rapidly when the dot-reservoir coupling is close to its critical value. Typically, the thermoelectric figure of merit ZT grows as the coupling approaches its critical value, but then drops sharply at the critical point.

I. INTRODUCTION

There is great current interest in the thermal and thermoelectric transport properties of quantum dots or molecules coupled to electronic reservoirs. It is known that they can be used as heat engines (converting a heat flow into electrical power) or refrigerators (using electrical power to extract heat from an already cold reservoir of electrons). Experimental demonstrations include Refs. [1–6], while much of the theory is reviewed in Ref. 7. However, few such works have considered the effects of the band structure of the electronic reservoirs on the quantum dot's transport properties, such as when the reservoirs are semiconductors with a band gap. Here we ask how the physics changes when the dot level is at an energy close to a band edge in the electronic reservoirs. As a first step in answering this question, we consider a non-interacting model, often known as the Fano-Anderson model,^{8,9} for which one can exactly solve the dynamics and extract all observables.

The bosonic version of the Fano-Anderson model with band edges has been extensively studied in the context of an atomic level coupled to a photonic continuum with a band structure. It has long been predicted that this model (and other similar models) exhibit an infinite-lifetime bound state,^{10–14} reviewed in Refs. 15 and 16. The state in the level get partially trapped in this bound state, and never fully decays into the continuum. This was recently observed in an NV centre in a waveguide,¹⁷ and is predicted to lead to various effects such as light-trapping¹⁸ and perfect subradiance.¹⁹ In the context of a quantum dot coupled to a superconductor, it leads to Landau-Zener-Stueckelberg physics.²⁰

If the continuum's density of states vanishes at the band gap, there is a transition from a situation without a bound state to one with a bound state, as the level's coupling to the continuum is increased.^{14,21,22} Qualitatively, the critical coupling at which this transition occurs is of order the energy difference between the level and reservoir's band edge. We consider this transition for a quantum dot coupled to two reservoirs, and ask

how the appearance of the infinite-lifetime bound state affects the dot's occupation and transmission function.

We start by showing that the appearance of the bound state corresponds to a transition in dot occupation from finite time correlations to infinite time correlations. We then turn to transport properties determined by the dot's transmission function. One might guess that the transition does not affect the transport properties, since an infinite-lifetime bound state cannot carry any current. However, we show that the dot's transmission function acquires singular properties at the transition, which leads to rapid changes in the electrical conductivity G , thermal conductivity C , and Seebeck coefficient, S . We discuss the consequences of this for the system's thermoelectric figure of merit, ZT . This thermoelectric response is very different from that without band gaps,^{23,24} where there is never a bound state.

Neither the bound state nor the transition are captured by the standard “weak-coupling” theory reviewed in Chapters 8 and 9 of Ref. 7; this shows the importance of developing strong-coupling theories to capture such physics. This work is a first step in this direction.

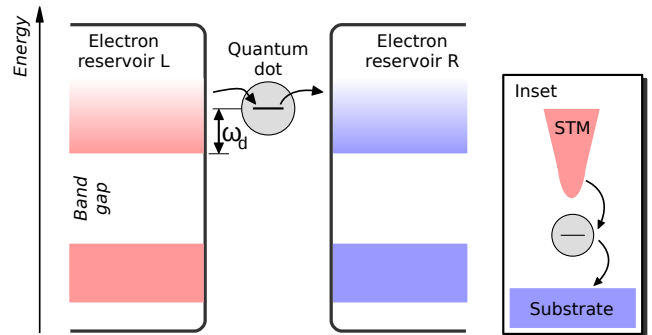


FIG. 1. A sketch of the type of system considered here, a single-level quantum dot between two semiconductor reservoirs. Inset: To study the system dynamics as a function of the dot-reservoir coupling, one can place the dot in a STM geometry as shown (or a break junction).

A. Contents of this work

Sections II-IV give the model and its formal exact solution. Sections V and VI respectively discuss the dot occupation for a sudden turn-on of the dot-reservoir couplings (quench) and an adiabatic turn-on. Section VII gives the transmission from reservoir L to R as a function of energy and coupling. Section VIII gives a hand-waving interpretation of these results in terms of a Lamb shift induced by level-repulsion. Section IX gives the electric and thermoelectric response, showing how sensitive it is to the dot-reservoir coupling.

II. THE MODEL

The Hamiltonian we study describes a single-level quantum dot coupled to two reservoirs,²⁵

$$\hat{H} = \omega_d \hat{d}^\dagger \hat{d} + \sum_{\alpha,k} \omega_{\alpha k} \hat{c}_{\alpha k}^\dagger \hat{c}_{\alpha k} + \sum_{\alpha,k} \left(g_{\alpha k} \hat{d}^\dagger \hat{c}_{\alpha k} + g_{\alpha k}^* \hat{c}_{\alpha k}^\dagger \hat{d} \right), \quad (1)$$

where \hat{d} and $\hat{c}_{\alpha k}$ denote field operators for an electron on the dot and in mode k of reservoir $\alpha \in \{L, R\}$ respectively; the corresponding energies are ω_d and $\omega_{\alpha k}$. Finally, $g_{\alpha k}$ describes the coupling between the dot and mode k in reservoir α . This model neglects electron-electron interactions on the dot. The simplest experimental implementation of such a model is to consider an interacting quantum dot (described by an Anderson impurity Hamiltonian) with a large enough magnetic field that the dot's spin-state with higher energy is always empty, which makes the on-dot interaction term negligible. The electron reservoirs contain infinitely many modes described by continuous spectral densities:

$$J_\alpha(\omega) = \sum_{\alpha,k} |g_{\alpha k}|^2 \delta(\omega - \omega_{\alpha k}). \quad (2)$$

Crucially we do *not* take the wide-band limit, and instead consider the case where the dot level is close to a band edge. The results in this work that explicitly contain $J_L(\omega)$, $J_R(\omega)$, or $J(\omega) = J_L(\omega) + J_R(\omega)$ are for an arbitrary band structure in the reservoirs (possibly with multiple bands and band gaps). However, we will particularly consider reservoirs with a single band, when the dot-level is close to the lower band edge. The reservoir's spectral density goes like a power law at this band edge, ω^s , and is regularised with exponential decay at high energies. In this case, we restrict our interest to two reservoirs made of the same material in the linear-response regime,²⁶ so

$$J_L(\omega) = J_R(\omega) = \begin{cases} \frac{K}{2} \left(\frac{\omega}{\omega_c} \right)^s e^{-\omega/\omega_c} & \text{for } \omega > 0, \\ 0 & \text{for } \omega < 0, \end{cases} \quad (3)$$

where (without loss of generality) we take the zero of energy to be the band edge.

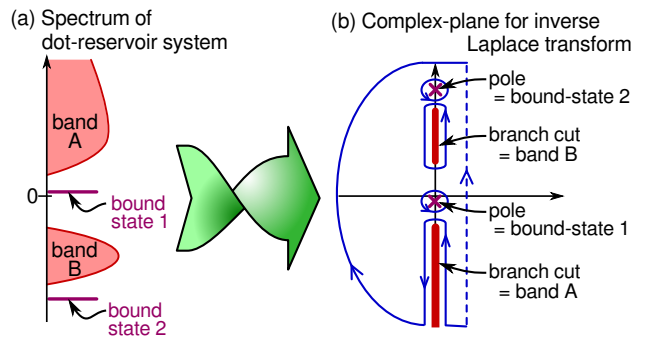


FIG. 2. An example of the correspondence between (a) the spectrum of Eq. (1) and (b) structures on the imaginary axis in the inverse Laplace transform, $\varphi(t)$. A bound state in the spectrum at energy ω_{*n} corresponds to a pole in the complex plane at $z = -i\omega_{*n}$. A band from energy ω to energy ω' corresponds to a branch cut from $z = -i\omega$ to $z = -i\omega'$. The inverse Laplace transform is an integral along the dashed blue contour in (b), which is deformed into the solid blue contour for evaluation.

III. SOLUTION VIA LAPLACE TRANSFORM

The Hamiltonian in Eq. (1) being quadratic, the Heisenberg equations of motion consist of a set of linear first-order differential equations. These are solved using the Laplace transform

$$\hat{D}(z) = \int_0^\infty dt e^{zt} \hat{d}^{(H)}(t), \quad (4)$$

where the operator is time-dependent because we work in the Heisenberg picture. In Laplace space, the dot annihilation operator satisfies

$$\hat{D}(z) = \frac{1}{z + i(\omega_d + \Sigma(z))} \left(\hat{d}_0 - i \sum_{\alpha,k} \frac{g_{\alpha k}}{z + i\omega_{\alpha k}} \hat{c}_{\alpha k;0} \right), \quad (5)$$

where \hat{d}_0 and $\hat{c}_{\alpha k;0}$ are the operators at time $t = 0$. The prefactor contains the self-energy

$$\Sigma(z) = \sum_{\alpha,k} \frac{|g_{\alpha k}|^2}{iz - \omega_{\alpha k}} = \int d\omega \frac{J(\omega)}{iz - \omega}, \quad (6)$$

where $J(\omega) = J_L(\omega) + J_R(\omega)$. For the spectral densities Eq. (3) this is

$$\Sigma(z) = -K\Gamma(1+s) \left(-\frac{iz}{\omega_c} \right)^s \Gamma \left(-s, -\frac{iz}{\omega_c} \right) e^{-iz/\omega_c}, \quad (7)$$

where $\Gamma(a)$ and $\Gamma(a, w)$ respectively denote the complete and incomplete Gamma functions.

IV. INVERSE LAPLACE TRANSFORM

The time-dependence of the dot's state is given by the inverse Laplace transform of Eq. (5). This is a product

of two terms, so the inverse Laplace transform is a convolution in time domain of the inverse Laplace transform of each term. The inverse transform of the expression in brackets in Eq. (5) is straight-forward, and we therefore focus on the prefactor. We define $\varphi(t)$ as the inverse Laplace transform of this prefactor,²⁷ $1/(z+i(\omega_d+\Sigma(z)))$. It is given by an integration along a vertical line in the complex plane, which we close as in Fig. 2b. This process leads to a solution in two parts: the first being the integral along the branch cuts, and the second coming from poles of Eq. (6). We will see that the branch cuts correspond to the continuum of states, while the poles correspond bound states in the band gaps.

The branch cut is always present, while the poles are only there if $z + i(\omega_d + \Sigma(z)) = 0$ has a solution. It is straightforward to show that any such solution is purely imaginary and so is given by the (real) zeros of the function

$$\Omega(\omega) = \omega - \omega_d - \int d\omega' \frac{J(\omega')}{\omega - \omega'}. \quad (8)$$

The zeros of $\Omega(\omega)$ only occur at values of ω where $J(\omega) = 0$, otherwise the integral in Eq. (8) is divergent, which means poles only occur at energies in the band gaps of the reservoirs.

The poles given by the zeros of $\Omega(\omega)$, can be shown to correspond to eigenstates of the full Hamiltonian for the dot coupled to the reservoirs, see Eq. (1). To see this, one must perform a Bogoliubov transformation on Eq. (1), so it takes the form of an arrowhead matrix, whose eigenvalues are given in Ref. 28. Upon taking the continuum limit, the surviving eigenvalues (those that do not fall in the continuum) are seen to satisfy $\Omega(\omega) = 0$. Thus the poles in the inverse Laplace transform correspond to eigenstates of Eq. (1) in the band gaps. These eigenstates are combinations of dot and reservoir states, and are usually called bound states because they do not decay into the continuum.¹³ Since $\Omega(\omega)$ is an increasing function of ω in any band gap, there is *at most* one bound state (pole) per band gap.

The case in Eq. (3) has a single band gap (which extends over all negative energies), it thus features *at most* one bound state. It has $\Omega(-\infty) = -\infty$, with $\Omega(\omega)$ monotonically increasing for $\omega < 0$, so the bound state exists in the band gap if and only if $\Omega(\omega \rightarrow 0^-) > 0$. Given Eq. (3), this criterion becomes $K > K_*$, where the critical coupling^{14,22}

$$K_* = \begin{cases} 0 & \text{for } s \leq 0, \\ \omega_d/\Gamma(s) & \text{for } s > 0. \end{cases} \quad (9)$$

For $s < 0$ (for example a square-root divergence in the density of states at the band edge) the bound state is present at all couplings. In contrast for all $s > 0$, there is no bound state at weak coupling, but one appears at a transition when one increases the coupling to $K = K_*$. The critical coupling, K_* , is proportional to the energy gap ω_d between the dot level and the band edge, hence

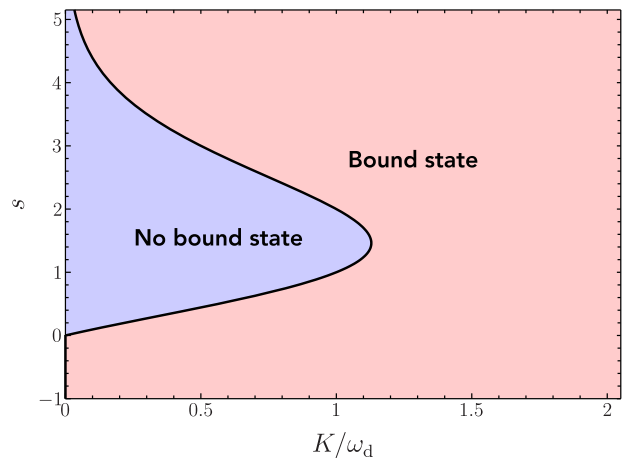


FIG. 3. Diagram showing the two possible regimes for a system with the spectrum in Eq. (3), as a function of the coupling parameter and scaling exponent. The blue and red domains respectively represent the low and high-coupling regimes. A bound state out of the continuum appears when the coupling exceeds its critical value (black line).

the transition will be easily observed in systems with the dot level close to the band edge. In contrast, the wide-band limit corresponds to the dot level infinitely far from any band edge, so one will not see a bound state for any finite dot-reservoir coupling.

In general one finds that

$$\varphi(t) = \int_{\text{B}} d\omega S(\omega) e^{-i\omega t} + \sum_n Z_{*n} e^{-i\omega_{*n} t}, \quad (10)$$

where \int_{B} in the first term is an integral over all bands (all ω where $J(\omega) \neq 0$) and is due to the continuum of states (branch cuts), while the second term is a sum over all bound states (poles). Eq. (10) introduces two quantities, Z_{*n} and $S(\omega)$. First, $Z_{*n} = |\langle \psi_{*n} | \hat{d}_0^\dagger | 0 \rangle|^2$ is the overlap between the dot-level and the n th bound state with energy ω_{*n} . It reads

$$Z_{*n} = \begin{cases} \left(1 + \int_0^\infty d\omega \frac{J(\omega)}{(\omega - \omega_{*n})^2} \right)^{-1} & \text{for } K > K_{*n}, \\ 0 & \text{for } K < K_{*n}. \end{cases} \quad (11)$$

where K_{*n} is the critical coupling above which the n th bound state appears. For the spectral density in Eq. (3), where there is only one bound state with critical coupling K_* given in Eq. (9), the precise nature of the discontinuity at $K = K_*$ is seen by taking $K - K_*$ to be small, then, for $0 < s < 1$,

$$Z_* = \begin{cases} \frac{\omega_c}{s} [B(s)]^{1/s} [\Gamma(s) (K - K_*)]^{(1-s)/s} & \text{for } K > K_*, \\ 0 & \text{for } K < K_*, \end{cases} \quad (12)$$

where $B(s) = \sin(\pi s)/(\pi K)$. For $s > 1$, we find that Z_* jumps to a finite value at the transition.

Secondly, the continuum contribution contains

$$S(\omega) = \frac{J(\omega)}{(\omega - \omega_d - \Lambda(\omega))^2 + \pi^2 J(\omega)^2}, \quad (13)$$

where $\Lambda(\omega)$ corresponds to the Lamb shift which accounts for the renormalization of the dot level due to the coupling to the reservoirs. It is given by the Cauchy principal value integral,

$$\Lambda(\omega) = \mathcal{P} \int d\omega' \frac{J(\omega')}{\omega - \omega'}. \quad (14)$$

V. DOT DYNAMICS WITH AN INITIAL QUENCH

Here, we consider the dynamics of the dot occupation $n(t)$ for an initial a product state, with the dot in a chosen state and the reservoirs in a thermal state. This is natural when the system and reservoirs are initially decoupled, and we instantaneously turn on the coupling (a quench) at time $t = 0$. This is the situation considered for an atom coupled to a reservoir of photons in Ref. 13, and we find the same result. In the absence of the bound state, the dot state decays to a final state which is independent of the initial state. In contrast, in the presence of the bound state, the dot gets partially trapped in its initial state forever.

The state at the moment of the quench ($t = 0$) is

$$\hat{\rho}(t = 0) = \hat{p}_0 \otimes \hat{\rho}_{L,\text{eq}} \otimes \hat{\rho}_{R,\text{eq}}, \quad (15)$$

where \hat{p}_0 is the initial density matrix of the quantum dot and $\hat{\rho}_{\alpha,\text{eq}}$ is the equilibrium density matrix for reservoir α ,

$$\hat{\rho}_{\alpha,\text{eq}} = \frac{e^{-\beta_\alpha \sum_k (\omega_{\alpha k} - \mu_\alpha) \hat{c}_{\alpha k;0}^\dagger \hat{c}_{\alpha k;0}}}{\text{Tr} \left(e^{-\beta_\alpha \sum_k (\omega_{\alpha k} - \mu_\alpha) \hat{c}_{\alpha k;0}^\dagger \hat{c}_{\alpha k;0}} \right)}, \quad (16)$$

with β_α and μ_α denoting the inverse temperature and the chemical potential of reservoir α . The average number of electrons on the dot is

$$n(t) = \langle \hat{d}^\dagger(t) \hat{d}(t) \rangle_0. \quad (17)$$

The exact dynamics of the field operators derived above, provide a full solution of the model. So the occupation for any time is

$$n(t) = n_0 |\varphi(t)|^2 + \int_B d\omega J(\omega) F(\omega) |\psi(t, \omega)|^2, \quad (18)$$

where n_0 is the initial occupation of the dot. Here, $F(\omega) = \sum_\alpha J_\alpha(\omega) f_\alpha(\omega) / J(\omega)$, so it is the ‘‘average’’ of the Fermi functions $f_L(\omega)$ and $f_R(\omega)$. The two other functions are $\varphi(t)$ given in Eq. (10) and

$$\psi(t, \omega) = i \int_0^t dt' \varphi(t') e^{-i\omega(t-t')}. \quad (19)$$

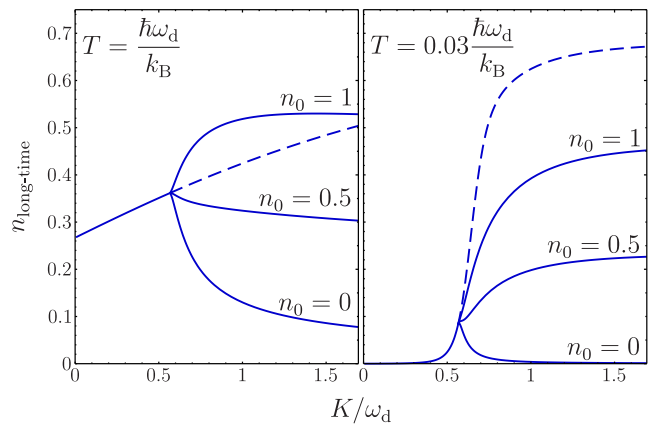


FIG. 4. Long-time dot occupation versus the system-reservoir coupling, K , when the two reservoirs have the same temperature and bias. The $J(\omega)$ for this plot is Eq. (3) with $\omega_c = 10\omega_d$, $s = 1/2$, $\mu = -0.01\omega_d$. The solid lines representing the occupation a long-time after a quench, Eq. (21), and exhibit a clear change of behaviour for $K = K_* \simeq 0.564\omega_d$. When $K > K_*$, the occupation at arbitrarily long times depends on the dot’s initial occupations, n_0 . The dashed lines are the occupation a long time after an adiabatic preparation, Eq. (28), and do not show the transition.

The long-time limit of $n(t)$ can be inferred using the Riemann-Lebesgue lemma which states that the Fourier transform of an integrable function vanishes at infinity. Then¹³

$$\varphi(t \rightarrow \infty) = \sum_n Z_{*n} e^{-i\omega_{*n}t}. \quad (20)$$

It is straightforward to obtain the long-time limit of $n(t)$ using arguments of this type, but in general the result is long and ugly. Appendix A shows that, in any situation with only one bound state, we can make use of the conservation of particle number^{29,30} to find a compact expression for the long-time limit of the dot occupation

$$n_{\text{long-time}} = \int_0^\infty d\omega S(\omega) F(\omega) + Z_*^2 \left(n_0 + \int_0^\infty d\omega \frac{J(\omega) F(\omega)}{(\omega - \omega_*)^2} \right). \quad (21)$$

One sees that when a bound state exists, $Z_* \neq 0$, the long-time occupation depends on the initial dot occupation, n_0 , because the dot gets partially trapped in its initial state forever. This is seen in Fig. 4, where the dot occupation a long time after a quench depends on the choice of n_0 for all $K > K_*$.

VI. DOT DYNAMICS WITH ADIABATIC PREPARATION

In quantum-dot or molecular nano-structures a rapid quench of the dot-reservoir coupling can be difficult. At

the same time the bound state will not have entirely infinite lifetime, because weak inelastic scattering effects (phonons, etc) which are beyond Eq. (1), will give it a long but finite lifetime. Thus, it is natural to consider an initial state which has had non-zero dot-reservoir coupling for so long that even the bound state has relaxed to its steady state by time t . This is equivalent to the adiabatic turn-on of the dot-reservoir couplings in the very distant past.³¹

With this initial condition, the dot occupation shows no discontinuity at the transition, see the dashed line in Fig. 4. However, we will show that the transition is visible as a discontinuity in the time-correlations of the dot occupation. In the absence of the bound state, the correlation between the occupation at time t and time $t + \tau$ decay with τ on a timescale given by the dot-reservoir coupling. In the presence of the bound state, this correlation acquires a component which is infinite range in τ . This is the equivalent of the non-decaying states discussed in Ref. 13 in the absence of the quench.

The correlation function that we consider is

$$G(t, \tau) = \langle \hat{n}(t + \tau) \hat{n}(t) \rangle_0 - \langle \hat{n}(t + \tau) \rangle_0 \langle \hat{n}(t) \rangle_0, \quad (22)$$

for large enough time that the system has achieved its steady state at time t , from the product state, $\hat{\rho}_0$, at time $t = 0$. To ensure that the bound state (if it exists) arrives at its steady state by time t , we add a small constant η to the coupling $J(\omega)$, so we replace $J(\omega)$ by

$$\tilde{J}_\alpha(\omega) = J_\alpha(\omega) + \eta \kappa_\alpha \quad (23)$$

in all quantities (indicating them with a tilde). For small but finite η , the bound state is replaced by a resonance, which gives a narrow Lorentzian in the density of states. This is a crude way of mimicking the weak inelastic effects that will give the bound state a finite lifetime, but will be sufficient for our purposes. The Lorentzian tends to a delta-function as $\eta \rightarrow 0$, and the resonance tends to an infinite lifetime bound state. As $\tilde{J}(\omega)$ represents a continuum extending over the whole range of frequencies, the formulae derived before can be used here upon extending the integrations to all frequencies, and dropping the Z_* -terms. At the end of the calculation, we take $t \rightarrow \infty$ and then $\eta \rightarrow 0$, to recover the physics of the bound state (including the Z_* term) between time t and $t + \tau$ while ensuring that even the bound state was completely relaxed to its steady state at time t .

In this situation the self-energy is

$$\tilde{\Sigma}(x - i\omega) = \Sigma(x - i\omega) - i\pi\eta(\kappa_L + \kappa_R) \text{sgn}(x). \quad (24)$$

The Lamb shift is unchanged as the additional term in the self-energy is purely imaginary. The steady-state occupation ($t \rightarrow \infty$) for finite η reads

$$\tilde{n}_{\text{long-time}} = \int_{\text{B}} d\omega \tilde{S}(\omega) \tilde{F}(\omega). \quad (25)$$

We now take the limit $\eta \rightarrow 0$. Crucially in the regimes where $J(\omega) = 0$ the limits are

$$\lim_{\eta \rightarrow 0} \tilde{F}(\omega) = \frac{\kappa_L f_L(\omega) + \kappa_R f_R(\omega)}{\kappa_L + \kappa_R}, \quad (26)$$

$$\lim_{\eta \rightarrow 0} \tilde{S}(\omega) = \sum_n Z_{*n} \delta(\omega - \omega_{*n}). \quad (27)$$

This yields for $\eta \rightarrow 0$

$$\tilde{n}_{\text{long-time}} = \int_{\text{B}} d\omega S(\omega) F(\omega) + \sum_n Z_{*n} F(\omega_{*n}), \quad (28)$$

which is a continuous function of dot-reservoir coupling (see e.g. the dashed line in Fig. 4).

The correlation function for $t \rightarrow \infty$ with finite η , reads

$$\tilde{G}(\tau) = \int d\omega d\omega' \tilde{F}(\omega) (1 - \tilde{F}(\omega')) \tilde{S}(\omega) \tilde{S}(\omega') e^{i(\omega - \omega')\tau}. \quad (29)$$

Taking the limit $\eta \rightarrow 0$ and then the limit of large τ , we find for any situation with only one bound state that

$$G_{\text{long-time}} = Z_*^2 F(\omega_*) (1 - F(\omega_*)). \quad (30)$$

We recall that Z_* in Eq. (11) is zero for dot-system coupling $K < K_*$ and non-zero for $K > K_*$. Thus the correlation decay if there is no bound state ($K < K_*$), so $G_{\text{long-time}}$ is zero. However when the bound state is present, then the correlations remain for all τ (up to the inelastic timescale).

For multiple bound states, $\tilde{G}(\tau)$ decays at large τ to coherent oscillations, due to beating between with different bound states,

$$G_{\text{long-time}} = \sum_{n,m} Z_{*n} Z_{*m} F_{*n} (1 - F_{*m}) e^{i(\omega_{*n} - \omega_{*m})\tau}, \quad (31)$$

where we write $F(\omega_{*n})$ as F_{*n} for compactness. This is reminiscent of the decay of a driven-dissipative classical system to a limit cycle, although here the oscillations in the long-time limit are of quantum origin.

The results in Eqs. (28,30) were originally found by one of us (M. H.) using the Keldysh field theory methods in Ref. 32.

Of course, the weak inelastic effects will cut-off the correlations induced by the bound state at the timescale of the inelastic scattering. However, at low temperatures this can be orders of magnitude longer than the timescale for decay in the absence of the bound state.

VII. TRANSPORT PROPERTIES

The bound state does not decay, which means that it cannot carry any current. Thus, one might expect that the presence or absence of this bound state has no effect on the transport properties of the dot. Thus the long-time transport properties, which are relevant to DC

transport and steady-state heat-engine physics, do not depend on the initial dot occupation. None the less, we will show that the transition at which the bound state appears does have an effect on the dot's transport properties.

The particle current into reservoir α is defined as

$$j_{\alpha}^{(N)}(t) = \frac{d}{dt} \sum_k \langle \hat{c}_{\alpha k}^{\dagger}(t) \hat{c}_{\alpha k}(t) \rangle_0. \quad (32)$$

Then at time t after a quench,

$$\begin{aligned} j_{\alpha}^{(N)}(t) = 2 \operatorname{Im} & \left(n_0 \varphi^*(t) \int d\omega J_{\alpha}(\omega) \psi(t, \omega) \right. \\ & + \int d\omega J_{\alpha}(\omega) f_{\alpha}(\omega) \psi^*(t, \omega) e^{-i\omega t} \\ & + \int d\omega d\omega' J_{\alpha}(\omega) J(\omega') F(\omega') \\ & \left. \times \psi^*(t, \omega') \chi(t, \omega, \omega') \right), \end{aligned} \quad (33)$$

where we have defined

$$\chi(t, \omega, \omega') = i \int_0^t dt' \psi(t', \omega') e^{-i\omega(t-t')}. \quad (34)$$

These currents do not cancel ($j_{\text{L}}^{(N)}(t) + j_{\text{R}}^{(N)}(t) \neq 0$), while the dot occupation is changing with time. However, in the steady state, particle conservation allow us to define, $j_{\text{steady}}^{(N)} = j_{\text{R}}^{(N)}(t \rightarrow \infty) = -j_{\text{L}}^{(N)}(t \rightarrow \infty)$. The steady state current is derived through the same process that led to the long-term occupation probability. After some algebraic manipulations, see the appendix, we find that this steady-state current takes a Landauer form^{24,33}

$$j_{\text{steady}}^{(N)} = \int_{-\infty}^{\infty} \frac{d\omega}{2\pi} \mathcal{T}(\omega) (f_{\text{L}}(\omega) - f_{\text{R}}(\omega)), \quad (35)$$

with the transmission function

$$\mathcal{T}(\omega) = \frac{4\pi^2 J_{\text{L}}(\omega) J_{\text{R}}(\omega)}{(\omega - \omega_{\text{d}} - \Lambda(\omega))^2 + \pi^2 J(\omega)^2}, \quad (36)$$

for all ω with non-zero $J_{\text{L,R}}(\omega)$. Here $\Lambda(\omega)$ is the Lamb shift defined in Eq. (14). This result does not depend on the initial state, and is the same for long times after a quench or adiabatic preparation.

The energy current entering reservoir α is defined as

$$j_{\alpha}^{(E)}(t) = \frac{d}{dt} \sum_k \omega_{\alpha k} \langle \hat{c}_{\alpha k}^{\dagger}(t) \hat{c}_{\alpha k}(t) \rangle_0. \quad (37)$$

With suitable algebraic manipulations, very similar to the ones of the particle current, we find that the steady-state energy current from L to R also takes a Landauer form,

$$j_{\text{steady}}^{(E)} = \int_{-\infty}^{\infty} \frac{d\omega}{2\pi} \omega \mathcal{T}(\omega) (f_{\text{L}}(\omega) - f_{\text{R}}(\omega)). \quad (38)$$

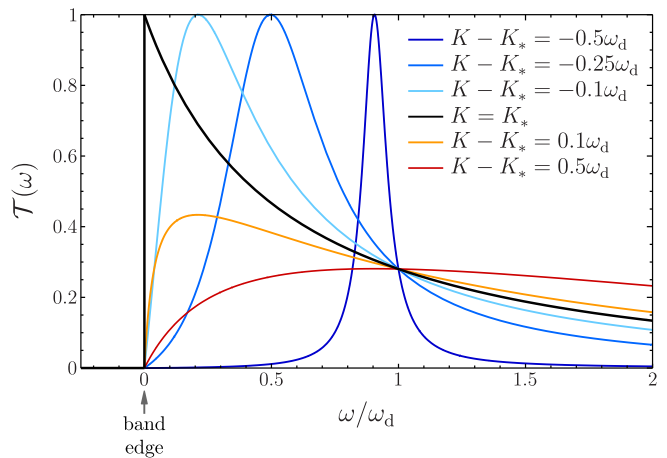


FIG. 5. Transmission as a function of frequency for various values of the coupling, when $J(\omega)$ is given by Eq. (3) and vanishes at the band edge. The parameters are $\omega_c = 10\omega_{\text{d}}$ and $s = 1/2$. For K much less than K_* (blue lines), the transmission function is a Lorentzian at the dot level. It then loses its shape and drifts towards the origin as the coupling increases up to its critical value (black line). When K exceeds K_* (light and dark orange lines), the transmission function becomes much flatter.

Thus the transport properties can be understood by studying the properties of the transmission function in Eq. (36). Fig. 5 shows the typical behaviour of the transmission function for different couplings K , when the spectral function is Eq. (3) with $0 < s < 1$. The transition can be clearly seen as a discontinuity of the transmission at the band edge, $\mathcal{T}(\omega \rightarrow 0^+)$, as a function of K . The nature of the discontinuity at small ω depends on the exponent s . For $0 < s < 1$, the low-frequency transmission is

$$\mathcal{T}(\omega \rightarrow 0^+) = \begin{cases} \frac{\pi^2 K^2 (\omega/\omega_c)^{2s}}{\Gamma^2(s)(K - K_*)^2} & \text{for } K \neq K_*, \\ \sin^2(\pi s) & \text{for } K = K_*. \end{cases} \quad (39)$$

Thus the transmission at the band edge has a discontinuity at $K = K_*$; it vanishes at the band edge for all $K \neq K_*$, but is finite for $K = K_*$. Indeed when $s = 1/2$ and $K = K_*$, the transmission at the band edge is perfect; $\mathcal{T}(\omega \rightarrow 0^+) = 1$. While the transmission is only a discontinuous function of K at $\omega \rightarrow 0^+$, it changes rapidly close to the transition for any $\omega \ll \omega_{\text{d}}$ (as seen in Fig. 5). For $s > 1$, we also find that the low-frequency behaviour of the transmission is different for $K \neq K_*$ and $K = K_*$, however, $\mathcal{T}(\omega)$ vanishes at the band edge in both cases.

In contrast, the behaviour is very different when $J(\omega)$ diverges at the band edge; $s < 0$ in Eq. (3). In this case there is a bound state at all values of the coupling, and the transmission *always* exhibits a peak at the band edge as we have $\mathcal{T}(\omega) \xrightarrow{\omega \rightarrow 0^+} \sin^2(\pi s)$. This result holds for any coupling, see for example Fig. 6. Thus even for very small coupling, where one would guess that the transmission

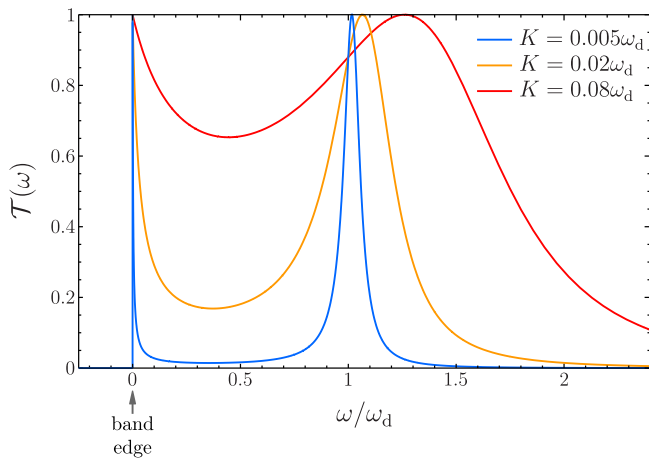


FIG. 6. Transmission as a function of frequency for various values of the coupling, when $J(\omega)$ is given by Eq. (3) and diverges at the band edge. The parameters taken for these plots are $\omega_c = 10\omega_d$ and $s = -1/2$. In this case the transmission has a peak at the band edge, irrespective of the value of the coupling. At small couplings the transmission looks like a Lorentzian at the dot-level ($\omega = \omega_d$), with an additional peak at the band edge ($\omega = 0$).

would be a narrow Lorentzian centred at the dot-level, there is a second narrow peak at the band edge.

VIII. INTERPRETATION AS A LAMB SHIFT

To get an more intuitive feel for the physics, this section describes the physics qualitatively by interpreting the Lamb shift in terms of level-repulsion between the dot level and the reservoir's continuum.

In this weak coupling limit, Fermi's golden rule tells us that the coupling to a continuum has two effects on the discrete levels of a quantum system. Firstly, the coupling shifts the energies of the discrete levels; this is known as a Lamb shift. Secondly the levels are broadened to become resonances because the state acquires a finite lifetime. The usual weak-coupling (Fermi golden rule) formula for the Lamb shift of the quantum dot level is $\Lambda(\omega_d)$, with $\Lambda(\omega)$ given in Eq. (14). This fits with the exact result in Eq. (14) when the coupling is weak enough that the physics is dominated by $\omega \simeq \omega_d$.

The Lamb shift has the following hand-waving interpretation in terms of the level repulsion between the dot level and individual continuum levels. The coupling to a continuum level with higher energy than the dot level will shift the dot level down in energy (with the continuum level being shifted up slightly). At the same time, the coupling to a continuum level with lower energy than the dot level will shift the dot level up in energy. The Lamb shift is the sum of all of these small shifts. If the continuum has a constant density of states (wide band limit), then the shifts up and down cancel, and there is no Lamb shift. However, if the continuum has a higher

density of states above the dot level than below it (as for Eq. (3) with $s > 0$), the Lamb shift is negative and moves the dot level to lower energies.

The transmission given in Eq. (36) has a peak at $\omega = \omega_d - \Lambda(\omega)$. For $s > 0$, as in Fig. 5, this peak moves to lower energies as the coupling is increased (for $K < K_*$). This corresponds to an increasingly negative Lamb shift of the dot level, which the coupling also gives a finite lifetime, broadening it into a resonance. When the coupling reaches the critical value K_* , the peaks sits exactly at the band edge, so at this and only this coupling, the transmission at the band edge is finite. When the coupling K becomes larger than K_* the Lamb shift is so large that it has moved the peak out of the band. One can naively interpret this as the Lamb shift having pushed the dot level out of the band, at which point the level becomes a bound-state with energy given by the ω which satisfies $\Omega(\omega) = 0$ in Eq. (8). However, more precisely, the dot state is then a superposition of the bound state and continuum states, so there is still transmission through the dot at $K > K_*$, but it no longer exhibits a peak with transmission equal to one.

This handwaving argument works less well for $s < 0$, because the usual weak-coupling (Fermi golden rule) argument does not reproduce the bound-state that is always present in the exact solution. However, the hand-waving argument at least gives an indication of why the transmission peak at $\omega = \omega_d$ in Fig. 6 moves to higher energies as the coupling is increased. This is because the Lamb shift is positive when the density of states is large below the dot level than above it. At the same time, there is another peak at the band-edge; this is because $J(\omega \rightarrow 0) \rightarrow \infty$, so Eq. (36) takes a finite value at $\omega = 0$ irrespective of the value of the $(\omega - \omega_d - \Lambda(\omega))^2$ -term in the denominator at $\omega = 0$.

IX. THERMOELECTRIC TRANSPORT COEFFICIENTS

When the differences in temperature and chemical potential between the two reservoirs are small compared to their average values, the linear response theory can be applied and all the transport properties of the system can be deduced from the thermoelectric transport coefficients.⁷ Taking the linear-response regime of Eqs. (35) and (38), one finds that the following thermoelectric quantities

$$\text{electric conductance, } G = e^2 I_0, \quad (40a)$$

$$\text{thermal conductance, } C = \frac{1}{T} \left(I_2 - \frac{I_1^2}{I_0} \right), \quad (40b)$$

$$\text{Seebeck coefficient, } S = \frac{I_1}{eT I_0}, \quad (40c)$$

$$\text{dimensionless figure of merit, } ZT = \frac{I_1^2}{I_0 I_2 - I_1^2}. \quad (40d)$$

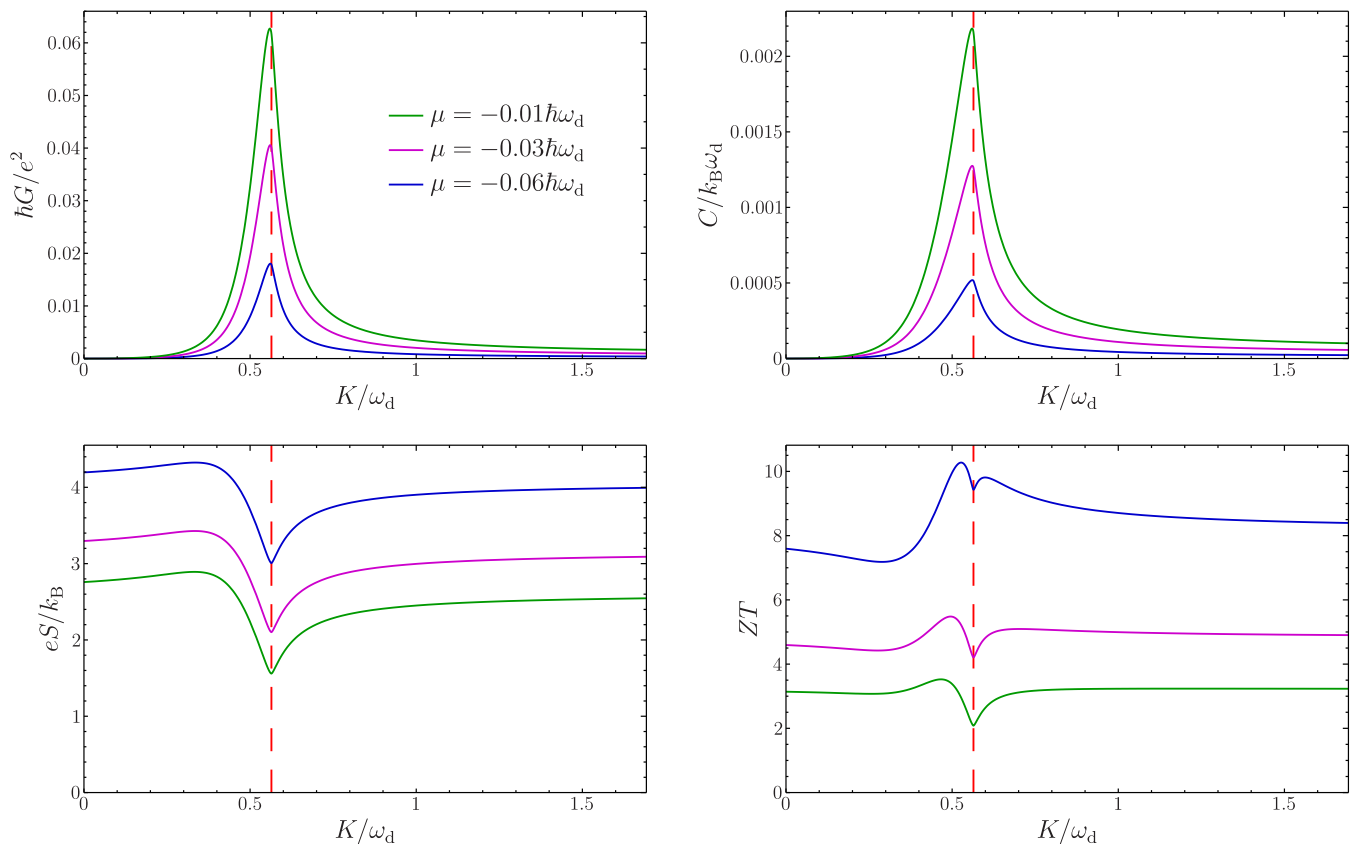


FIG. 7. Transport coefficients versus coupling for different values of the chemical potential. The parameters taken for these plots are $\omega_c = 10\omega_d$, $s = 1/2$, $T = 0.03\omega_d/k_B$. The dashed red vertical line indicates the critical coupling K_* , with $K_*/\omega_d \simeq 0.56$ for these parameters.

Here e is the electron charge, T is the average temperature of the two reservoirs ($T \simeq T_L \simeq T_R$), and

$$I_n = \int_{-\infty}^{\infty} \frac{d\omega}{2\pi} (\omega - \mu)^n \mathcal{T}(\omega) (-f'(\omega)), \quad (41)$$

with $f'(\omega)$ being the derivative of the Fermi distribution, $-f'(\omega) = (\beta/4) \cosh^{-2}(\beta(\omega - \mu)/2)$.

From these equations, we see that the change of behaviour of the transmission at low frequencies leads to rapid changes for the transport coefficients when one considers the electrochemical potential below the band edge ($\mu < 0$). Indeed, $-f'(\omega)$ is basically a box centered on μ of width $\sim T$ that is superimposed on the transmission function. If one then takes μ to be negative and T of the order of $|\mu|$, the transport coefficients will be dominated by the small ω behaviour of $\mathcal{T}(\omega)$. As the discontinuity in the transmission is only at $\omega = 0^+$, and these coefficients involves integrals over ω , they do not exhibit any discontinuities at $K = K_*$, but they carry a signature of the discontinuity in their rapid change with K . Fig. 7 shows this rapid change in electric and thermoelectric properties close to $K = K_*$; in some cases the change is so rapid, that the curve looks discontinuous. It only becomes strictly discontinuous in the $\mu \rightarrow 0$

and $T \rightarrow 0$ limit, which is also the limit where C and S become vanishingly small.

The conductances exhibit a peak at $K \simeq K_*$ whereas the Seebeck coefficient and the figure of merit (and thus the efficiency) typically drop at this point. The latter two have dips at $K \simeq K_*$, because of a competition between the peaks in their numerators and the peaks in their denominators; the denominator wins in all the cases we have looked at. In the limit $\mu \rightarrow 0$ and $T \rightarrow 0$, these peaks and dips become discontinuities in the derivative of the function in question, and sit exactly at K_* . These fast variations of transport coefficients with K typically lead to increased S and ZT near to the transition. For example in Fig. 7, ZT is almost 20% larger near the transition than at small coupling.

X. CONCLUSIONS

We consider the infinite-lifetime bound states of a quantum dot coupled to reservoirs with band gaps. For reservoir's spectra that vanish at the band edge, a bound state appears in the band gap when the dot-reservoir coupling exceeds a critical value. This transition induces a discontinuity in the dot's transmission at the band edge,

which can have a strong signature in the electric and thermoelectric transport properties.

For reservoir spectra that diverge at the band edge, there is a bound state for all coupling. The dot's transmission has a peak at the band edge, even at arbitrarily weak coupling. This peak will dominate transport whenever the electrochemical potential is close to the band edge. The usual argument, that the dot's transmission is a Lorentzian centred at the dot level, will give erroneous transport properties in such situations.

The richness of this model could not be guessed from the usual weak-coupling arguments, this suggests that other surprises may await us in the strong-coupling limit when we add electron-electron interactions.

ACKNOWLEDGMENTS

We thank D. Basko, M. Holzmann, N. Lo Gullo, and K. Saito for stimulating discussions and useful comments. This work was supported by the French ANR-15-IDEX-02 via the Université Grenoble Alpes QuEnG project.

Appendix A: Some details on the calculation of long-time occupation and current

We explain here how one can combine the Riemann-Lebesgue lemma and continuity equation to obtain the long-time limits of the dot occupation (Eq. (21)) and particle (Eq. (35)). We focus on situations with a single energy band for positive energies, that is, with only one bound state.

Using the same kind of arguments that gave $\varphi(t \rightarrow \infty)$ in Eq. (20), we obtain the following expression for the

long-time occupation,

$$n_{\text{long-time}} = \int_0^\infty d\omega J(\omega)A(\omega)F(\omega) + Z_*^2 \left(n_0 + \int_0^\infty d\omega \frac{J(\omega)F(\omega)}{(\omega - \omega_*)^2} \right). \quad (\text{A1})$$

For what follows, we have regrouped a number of terms in $A(\omega)$, defined as

$$A(\omega) = \sigma(\omega)^2 + \pi^2 S(\omega)^2 + \frac{2Z_*\sigma(\omega)}{\omega - \omega_*} + \frac{Z_*^2}{(\omega - \omega_*)^2}, \quad (\text{A2})$$

where $\sigma(\omega)$ is the following principal value integral,

$$\sigma(\omega) = \mathcal{P} \int d\omega' \frac{S(\omega')}{\omega - \omega'}. \quad (\text{A3})$$

Similarly, the steady-state currents read

$$j_\alpha^{(N)}(t \rightarrow \infty) = 2\pi \int_0^\infty d\omega J_\alpha(\omega)(J(\omega)A(\omega)F(\omega) - S(\omega)f_\alpha(\omega)). \quad (\text{A4})$$

It is straightforward to show that the quantum dot obeys the continuity equation

$$\frac{dn}{dt} + j_L^{(N)} + j_R^{(N)} = 0. \quad (\text{A5})$$

We see from Eq. (A1) that the occupation is constant in the limit $t \rightarrow \infty$. The steady-state currents thus cancel ($j_L^{(N)} + j_R^{(N)} = 0$) and we consequently find

$$\int_0^\infty d\omega J(\omega)F(\omega)(J(\omega)A(\omega) - S(\omega)) = 0. \quad (\text{A6})$$

In the integral of Eq. (A6), only the factor $F(\omega)$ depends on the temperatures and chemical potentials of the reservoirs. However, the aforementioned integral has to vanish for any choice of reservoirs. We thus understand that the integrand of Eq. (A6) necessarily cancels, that is

$$J(\omega)A(\omega) = S(\omega). \quad (\text{A7})$$

Then, replacing $A(\omega)$ in Eqs. (A1) and (A4), we obtain the simpler expressions in Eqs. (21) and (35).

* etienne.jussiau@lpmmc.cnrs.fr

† h.masahiro@issp.u-tokyo.ac.jp

‡ robert.whitney@grenoble.cnrs.fr

¹ P. Reddy, S.-Y. Jang, R. A. Segalman, and A. Majumdar, "Thermoelectricity in molecular junctions," *Science* **315**, 1568–1571 (2007).

² J. R. Prance, C. G. Smith, J. P. Griffiths, S. J. Chor-

ley, D. Anderson, G. A. C. Jones, I. Farrer, and D. A. Ritchie, "Electronic refrigeration of a two-dimensional electron gas," *Phys. Rev. Lett.* **102**, 146602 (2009).

³ J. Balachandran, P. Reddy, B. D. Dunietz, and V. Gavini, "End-group-induced charge transfer in molecular junctions: effect on electronic-structure and thermopower," *J. Phys. Chem. Lett.* **3**, 1962–1967 (2012).

- ⁴ H. Thierschmann, R. Sánchez, B. Sothmann, F. Arnold, C. Heyn, W. Hansen, H. Buhmann, and L. W. Molenkamp, “Three-terminal energy harvester with coupled quantum dots,” *Nat. Nanotechnol.* **10**, 854–858 (2015).
- ⁵ B. Roche, P. Roulleau, T. Jullien, Y. Jompol, I. Farrer, D. A. Ritchie, and D. C. Glattli, “Harvesting dissipated energy with a mesoscopic ratchet,” *Nat. Commun.* **6**, 6738 (2015).
- ⁶ F. Hartmann, P. Pfeffer, S. Höfling, M. Kamp, and L. Worschech, “Voltage fluctuation to current converter with Coulomb-coupled quantum dots,” *Phys. Rev. Lett.* **114**, 146805 (2015).
- ⁷ G. Benenti, G. Casati, K. Saito, and R. S. Whitney, “Fundamental aspects of steady-state conversion of heat to work at the nanoscale,” *Phys. Rep.* **694**, 1–124 (2017).
- ⁸ P. W. Anderson, “Localized magnetic states in metals,” *Phys. Rev.* **124**, 41 (1961).
- ⁹ U. Fano, “Effects of configuration interaction on intensities and phase shifts,” *Phys. Rev.* **124**, 1866 (1961).
- ¹⁰ S. John and J. Wang, “Quantum electrodynamics near a photonic band gap: Photon bound states and dressed atoms,” *Phys. Rev. Lett.* **64**, 2418 (1990).
- ¹¹ S. John and J. Wang, “Quantum optics of localized light in a photonic band gap,” *Phys. Rev. B* **43**, 12772 (1991).
- ¹² S. John and T. Quang, “Spontaneous emission near the edge of a photonic band gap,” *Phys. Rev. A* **50**, 1764 (1994).
- ¹³ A. G. Kofman, G. Kurizki, and B. Sherman, “Spontaneous and induced atomic decay in photonic band structures,” *J. Mod. Opt.* **41**, 353–384 (1994).
- ¹⁴ W.-M. Zhang, P.-Y. Lo, H.-N. Xiong, M. W.-Y. Tu, and F. Nori, “General non-Markovian dynamics of open quantum systems,” *Phys. Rev. Lett.* **109**, 170402 (2012).
- ¹⁵ D. G. Angelakis, P. L. Knight, and E. Paspalakis, “Photonic crystals and inhibition of spontaneous emission: an introduction,” *Contemp. Phys.* **45**, 303–318 (2004).
- ¹⁶ D. E. Chang, J. S. Douglas, A. González-Tudela, C.-L. Hung, and H. J. Kimble, “Colloquium: Quantum matter built from nanoscopic lattices of atoms and photons,” *Rev. Mod. Phys.* **90**, 031002 (2018).
- ¹⁷ Y. Liu and A. A. Houck, “Quantum electrodynamics near a photonic bandgap,” *Nat. Phys.* **13**, 48 (2017).
- ¹⁸ P. Longo, P. Schmitteckert, and K. Busch, “Few-photon transport in low-dimensional systems: Interaction-induced radiation trapping,” *Phys. Rev. Lett.* **104**, 023602 (2010).
- ¹⁹ A. González-Tudela and J. I. Cirac, “Quantum emitters in two-dimensional structured reservoirs in the nonperturbative regime,” *Phys. Rev. Lett.* **119**, 143602 (2017).
- ²⁰ D. M. Basko, “Landau-Zener-Stueckelberg physics with a singular continuum of states,” *Phys. Rev. Lett.* **118**, 016805 (2017).
- ²¹ G. Engelhardt, G. Schaller, and T. Brandes, “Bosonic Josephson effect in the Fano-Anderson model,” *Phys. Rev. A* **94**, 013608 (2016).
- ²² Y.-C. Lin, P.-Y. Yang, and W.-M. Zhang, “Non-equilibrium quantum phase transition via entanglement decoherence dynamics,” *Sci. Rep.* **6**, 34804 (2016).
- ²³ G. Schaller, *Open quantum systems far from equilibrium* (Springer, 2014).
- ²⁴ G. E. Topp, T. Brandes, and G. Schaller, “Steady-state thermodynamics of non-interacting transport beyond weak coupling,” *Europhys. Lett.* **110**, 67003 (2015).
- ²⁵ We measure energies in units of inverse time, so $\hbar = 1$.
- ²⁶ Electroneutrality means that each reservoir’s band structure is shifted in energy by e times the reservoir’s bias. Hence reservoirs made of the same material will *only* have the same spectral function in the limit where the bias is negligibly small (linear response regime).
- ²⁷ Physically, $\varphi(t)$ gives the time dependence of the average value of the annihilation operator $\hat{d}(t)$.
- ²⁸ D. P. O’Leary and G. W. Stewart, “Computing the eigenvalues and eigenvectors of symmetric arrowhead matrices,” *J. Comput. Phys.* **90**, 497–505 (1990).
- ²⁹ C. Caroli, R. Combescot, P. Nozières, and D. Saint-James, “Direct calculation of the tunneling current,” *J. Phys. C* **4**, 916 (1971).
- ³⁰ Y. Meir and N. S. Wingreen, “Landauer formula for the current through an interacting electron region,” *Phys. Rev. Lett.* **68**, 2512 (1992).
- ³¹ If the two reservoirs have the same T and μ , this steady state is the thermal state of the full Hamiltonian in Eq. (1).
- ³² M. Hasegawa and T. Kato, “Effect of interaction on reservoir-parameter-driven adiabatic charge pumping via a single-level quantum dot system,” *J. Phys. Soc. Jpn.* **87**, 044709 (2018).
- ³³ Rolf Landauer, “Spatial variation of currents and fields due to localized scatterers in metallic conduction,” *IBM J. Res. Dev.* **1**, 223–231 (1957).